Turbulent Burning Rates of Methane and Methane-Hydrogen Mixtures

M. Fairweather[†], M.P. Ormsby[‡], C.G.W. Sheppard[‡] and R. Woolley[¶]

[†]School of Process, Environmental and Materials Engineering, and [‡]School of
Mechanical Engineering, University of Leeds, Leeds LS2 9JT, UK

[¶]Department of Mechanical Engineering, University of Sheffield, Sheffield S1 3JD, UK

Corresponding Author for Review Process: Prof. M. Fairweather
School of Process, Environmental and
Materials Engineering
University of Leeds
Leeds LS2 9JT
UK

Tel: +44 (0) 113 343 2419
Fax: +44(0) 113 343 2405
Email: m.fairweather@leeds.ac.uk

Abstract

Methane and methane-hydrogen (10%, 20% and 50% hydrogen by volume) mixtures have been ignited in a fan stirred bomb in turbulence and filmed using high speed cine schlieren imaging. Measurements were performed at 0.1 MPa (absolute) and 360 K. A turbulent burning velocity was determined for a range of turbulence velocities and equivalence ratios. Experimental laminar burning velocities and Markstein numbers were also derived. For all fuels the turbulent burning velocity increased with turbulence velocity. The addition of hydrogen generally resulted in increased turbulent and laminar burning velocity and decreased the Markstein number. Those flames that were less sensitive to stretch (lower Markstein number) burned faster under turbulent conditions, especially as the turbulence levels were increased, compared to stretch-sensitive (high Markstein number) flames.

Keywords: turbulent premixed, laminar premixed, burning rates, measurement, methane, methane-hydrogen

Nomenclature

A, b / dimensionless   Constants

Da Damkholer number

f_s / r.p.m.   fan speed

K / dimensionless   Karlovitz stretch factor

L / m   integral length scale

$L_b, L_s, L_c, L_{sr}, L_{cr}$ / m   Markstein lengths

Le / dimensionless   Lewis number

Ma, Ma_{sr} / dimensionless   Markstein number

r_{sch} / m   schlieren flame radius

t / s   time from ignition

S_n / m s^{-1} stretched flame speed

S_s / m s^{-1} unstretched flame speed

u' / m s^{-1} r.m.s. turbulent velocity

u'_k / m s^{-1} effective r.m.s. turbulent velocity

u_l / m s^{-1} unstretched laminar burning velocity

u_n, u_{nr} / m s^{-1} stretched laminar burning velocities

u_t / m s^{-1} turbulent burning velocity

u_{te} / m s^{-1} turbulent burning velocity (entrainment)

u_{tr} / m s^{-1} turbulent burning velocity (conversion rate to products)

Greek Symbols

$\alpha, \alpha_s, \alpha_c$ / s^{-1} laminar stretch rates

δ_ℓ / m   laminar flame thickness

ϕ / dimensionless   equivalence ratio

λ / m   Taylor turbulent length scale

ρ_b / kg m^{-3} burned gas density

ρ_u / kg m^{-3} unburned gas density

ν / m^2 s^{-1} kinematic viscosity

1. Introduction

Hydrogen is a potential future energy carrier offering CO_2 free emissions at the point of combustion [1]. However, transition to the hydrogen economy is not straightforward and will require significant investment and technological development in the manufacture, transport and use of hydrogen. As a first step towards a hydrogen economy the NATURALHY project (see acknowledgements and http://www.naturalhy.net) is considering the potential for using the existing natural gas infrastructure as a means to transport hydrogen (mixed with natural gas) from manufacturing sites to end users. The mixture could then be used directly, or the hydrogen could be extracted and used in fuel cells or combusted. This strategy may assist hydrogen production and hydrogen fuelled application to become established more quickly than might otherwise be the case. However, existing gas customers would receive a natural gas-hydrogen mixture and this may have safety implications. Additionally, the gas infrastructure has been designed and operated on the basis that natural gas is the medium being conveyed. The addition of hydrogen to the network may also impact on safety.

Hydrogen is significantly more reactive than natural gas (which predominantly comprises methane) and when premixed with air its laminar burning velocity is approximately 5.8 times that of methane under stoichiometric conditions [2], with much wider flammability limits. It has been shown by a number of researchers that the laminar burning velocities of methane-hydrogen mixtures are greater than those of pure methane, e.g. [2, 3] and references therein. It is therefore necessary to identify and quantify the consequences and level of risk resulting from accidental releases (and subsequent ignition and fire or explosion) of natural gas-hydrogen mixtures during their transmission, storage, distribution and use. Such events are likely to be turbulent rather than laminar in nature. One means of assessing hazards is the use of mathematical models capable of predicting the consequences of accidental fires and explosions. For use in the formulation and validation of ignition and explosion models in particular, necessary inputs are measurements of laminar and turbulent burning velocities of natural gas (or methane)-hydrogen mixtures.

The turbulent burning velocity depends on the flow field (typically represented by the root mean square (r.m.s.) turbulent velocity and an eddy length scale) and the flame chemistry (the laminar burning velocity, laminar flame thickness and, sometimes, a Lewis/Markstein number). The temperature and pressure also influence both the flow field and flame chemistry. Expressions for these effects on u_t are often generalised in compact form, based on correlations using non-dimensional groups. These are sometimes given in terms of u_t/u' plotted against the Karlovitz stretch factor, K (or the Damkohler number), with K given by [4]:

$$K = \frac{u'\delta_l}{u_l\lambda},$$
(1)

where λ is the Taylor microscale of turbulence and δ_l the laminar flame thickness, defined here as ν/u_l. Both the Karlovitz and Damkohler numbers relate the chemical and turbulent eddy lifetimes.

The correlation which contains the largest amount of turbulent burning velocity data to date is that of Bradley *et al.* [4], comprising data from over 1600 measurements. The majority of these data relate to the stoichiometric fuel-air ratio, for a number of fuels, and atmospheric pressure. However, some of the data drawn from the available literature were poorly defined, resulting in significant scatter in the experimental data. Since generating this correlation, the importance of using a consistent definition of the turbulent burning velocity has become clear. A widely used definition of the turbulent burning velocity is that derived from the entrainment of fresh unburned gas into the flame, u_{te} [5]. However, Abdel-Gayed *et al.* [6] identified an alternative burning rate based on the conversion rate to burned products, u_{tr}; this burning velocity parameter relates more directly to pressure generation. After ignition a flame can only be wrinkled by those turbulent eddies smaller than itself. Eddies larger than the flame will convect it. As the flame grows it encompasses eddies of increasing size resulting in a thicker flame brush (the distance between completely burned products and unburned mixture). The

entrainment of fresh mixture occurs at the front of the flame, whilst the production of burned gas occurs in the middle of the brush, and as u_{tr} and u_{te} are associated with two different surfaces, and flame brush thickness changes with flame propagation, they often have different values.

The turbulent burning velocities reported here have been derived for expanding flames ignited in a turbulent field in which the mean velocity of the flow was zero in all directions, although the instantaneous velocity at any point and in any direction was continuously changing. The flames were imaged using high speed schlieren photography. Simultaneous laser sheet and schlieren measurements have been performed in the same vessel [7] for propane flames where it was demonstrated that the flame brush thickness continually increased (for all the flames monitored) from ignition till they passed beyond the windows. These earlier studies suggested that it was possible to determine the mass rate of burning, related to the turbulent burning velocity, u_{tr}, on the basis of high speed schlieren photography:

$$u_{tr} = \left(\frac{1}{1.11} \frac{\rho_b}{\rho_u} \right) \frac{dr_{sch}}{dt} ,$$ (2)

where ρ_b and ρ_u are the burned and unburned gas densities, respectively, with the burned gas density calculated using a chemical equilibrium program [8]. The schlieren derived mean flame radius in Eq. (2) is r_{sch}, and this equation is an empirically based expression obtained using a number of propane-air flames at different equivalence ratios, u' and pressures. Measurements were performed up to $u'/u_l = 10.7$. More recently, simultaneous measurements of schlieren imaging and the pressure rise in the vessel have been performed on a variety of fuels [9] and the turbulent burning velocity, u_{tr}, measured with the two techniques was shown to be similar up to $u'/u_l = 36$. In the present work, data used for u'/u_l in the final correlations do not exceed the latter value.

Schlieren photography was selected as the measurement method as it is a non-intrusive optical technique and is relatively easily applied. High speed laser sheet Mie

scattering imaging provides better definition of the flame surface, but requires the added complication of the addition of a seed at the appropriate concentration. In addition, at higher turbulent velocities it can become difficult to obtain a representative slice through the flame as the flame kernel can convect out of the plane of the sheet. In comparison, schlieren imaging is an integrated technique making it easier to track the flame progress. Measurements of the pressure rise are also non-intrusive and provide a direct measurement of the rate of production of burned gas [5]. However, the pressure rise is proportional to the enflamed volume and a pressure rise can only be detected with sufficient accuracy at relatively large flame radii. In the rig used here, the fans were situated within the vessel and so there was only a short time from a detectable pressure rise to the flame being disturbed by the fans.

A limited dataset of laminar and turbulent methane-hydrogen flames had previously been obtained at 0.5 MPa [10]. In this study, flames were ignited at $u' = 2$ m s^{-1} and the equivalence ratio varied between the fuel-lean to rich ignition limits. The addition of hydrogen increased the laminar burning velocity, particular at fuel-lean equivalence ratios. This trend continued to turbulent burning velocities, where it was shown that the addition of hydrogen had significant impact only for fuel-lean mixtures. This behaviour was contrasted with that of methanol (no effect of ϕ on u_{tr}) and iso-octane (turbulent fuel-rich ϕ faster than fuel-lean).

The experimental work reported here generated a database for the burning velocity of methane-hydrogen mixtures, with pure methane used in place of natural gas in the experiments due to the variability in the latter's composition. Work was undertaken at atmospheric pressure and with an initial temperature of 360 K, using both laminar mixtures and a range of turbulence velocities. Mixtures with air of pure methane, 90% CH_4-10% H_2, 80% CH_4-20% H_2 and 50% CH_4-50% H_2, by volume, were considered over the fuel-lean to rich ignition limits. The various fuels are referred to as CH_4, 10% H_2, 20% H_2 and 50% H_2 in the following text. The turbulent burning velocity data gathered are also presented in compact form, based on generalised correlations using non-dimensional groups, for subsequent use in explosion models.

2. Experimental Work

A 30 litre spherical stainless steel vessel was employed in the experiments. Three pairs of orthogonal quartz windows of diameter 150 mm provided optical access. Turbulence was generated in the bomb by four identical eight bladed fans in a symmetrical tetrahedral configuration. The fans were directly coupled to electric motors with separate speed controllers. Each fan was separately adjustable between 3.3 and 167 Hz (200 to 10,000 r.p.m.) and controlled by solid state variable frequency converter units. The individual fan speeds were set and maintained within ±5% of each other to attain the required turbulence intensity. The mean and r.m.s. velocities, and integral length scale, have been determined using laser Doppler velocimetry. Previous workers [11] found a central region of reasonably uniform isotropic turbulence in this vessel corresponding to the region of optical access (150 mm). Here the r.m.s. turbulence velocity, u', was found to be represented by

$$u' = 0.00119 f_s, \tag{3}$$

where f_s is the fan speed. This correlation was found valid for all operating pressures, temperatures and mixture viscosities. The integral length scale L was found by two-point correlation to be 20 mm and was independent of all operating variables [11].

Mixture temperature was measured using a K-type thermocouple, situated inside the chamber. The entire vessel was preheated by an internal 2 kW heater. A piezoresistive pressure transducer was employed to measure the pressure during mixture preparation. This transducer was situated outside the vessel and was isolated just prior to ignition.

Mixtures were prepared in the vessel, with gas concentrations set on the basis of partial pressures. After an experiment, the vessel was flushed with compressed air and then evacuated. Dry cylinder air was used in preparation of the combustible mixture. Fuel was supplied from high pressure cylinders containing set premixed methane-

hydrogen mixtures (supplied by BOC). The fans were run, at low speed, during charge preparation to ensure full mixing and to maintain uniform heating of the vessel from the heater. In turbulent flame experiments the fan speed was then adjusted to give the desired turbulence level, whilst in laminar flame experiments, following mixture preparation, the fans were switched off for at least 60 seconds before ignition; this allowed the mixture to become quiescent. An initial charge temperature of 360 K was adopted in all experiments; otherwise because of kinetic heating at high fan speeds, the vessel would have required cooling for burning mixtures at room temperature. The estimated precision in the equivalence ratio setting was ±0.04 in the value of ϕ, this being a function of temperature variation during vessel filling and the accuracy of the pressure transducers.

Ignition was initiated using a purpose built stainless steel/ceramic sparkplug, with a gap of 1 mm, mounted in the centre of the vessel. A Lucas 12 V transistorised automotive ignition coil system was connected to the spark electrode assembly. The average spark energy was measured to be 23 mJ [12]. For the extremes of fuel-rich conditions close to mixture flammability limits ($\phi > 1.2$ in the case of CH_4), a higher powered capacitance discharge ignition system (~300mJ) was used, as described in [13]. However, all burning velocities were measured at sufficiently large radii that spark effects could be neglected [14].

The flames were imaged using schlieren photography, employing a 20 W tungsten element lamp, 1 m focal length lenses and a pinhole. The schlieren images were captured using a Photosonics Phantom 9 camera framing at 2000 f.p.s. and 512×512 pixels for laminar flames, and up to 9000 fps and 386×386 pixels for turbulent flames. For $u' = 8$ and 10 m s^{-1} a resolution of 192×192 and framing rate of 20,000 fps was adopted. Shown in Fig. 1 are typical successive images of a developing turbulent flame observed in the study. Flames moved outwards from the spark consuming unburned gases. The resulting images were either hand traced or processed using Adobe PhotoShop 6.0. By subtracting the background (pre-explosion) image from the subsequent images and applying a threshold, a binary image was produced for each frame where the burned area was white

and the remainder black. The image of the spark plug was manually removed. Flame areas were then measured by counting the number of pixels behind the flame front. Flame radii were computed as those of a circle of area equal to that of the imaged flame.

The processing steps are illustrated in Fig. 2. Shown in Fig. 2 (c) is a typical image histogram after background subtraction for the flame given in Figs. 2 (a) and (b). The captured images were 8 bit, so grey levels from 0 (black, background) to 255 (white, flame) were processed. The threshold value was selected on the basis of visual inspection. If too low a value was selected, noise was clearly visible (a splatter of white pixels ahead of the flame), and as the value was increased, flame features were lost on the thresholded image. A typical range of possible threshold values is indicated on Fig. 2(c), the actual value chosen was around 14. Flame radius plotted against time from ignition is given in Fig. 2(d) for different threshold values. The flame radius continually increased with time from ignition for all the flames studied (unless the flame quenched, although this was only observed at small radii). The range of threshold values used here had little impact on the flame radius derived. The turbulent burning velocity, u_{tr}, is shown against time from ignition for different threshold values in Fig. 2(e). The turbulent burning velocity continually increased with time from ignition, with no levelling off in the burning velocity with time (or flame radius) observed in the flames studied. The selection of threshold value is shown not to have a strong impact on the burning velocity derived, except at the initial stages where the flames were small and the velocity sensitive to small changes in the processing method. This is demonstrated by the standard deviation in the burning velocity for the range of threshold values chosen, with the standard deviation high at small times but reducing as the time from ignition (and hence the flame radius) increased.

Turbulent flames were studied at stoichiometric conditions for all fuel mixtures at values of u' of 0.5, 1, 2, 4, 6, 8 and 10 m s^{-1}. The effect of equivalence ratio was studied between values set by the experimental ignition limits at both $u' = 2$ and 6 m s^{-1}. For each laminar condition, two repeat tests were performed; for turbulent cases five tests

were normally completed at each condition, although ten experiments were required for $u' > 6$ m s^{-1}.

Laminar burning velocities were obtained for each fuel over the range of equivalence ratios that could be ignited. Spherically expanding flames were filmed, and the resulting flame radius vs. time data processed to yield u_l and Markstein numbers. Further details can be found in [14] and [15]. Using spherically expanding flames the influence of flowfield stretch on the laminar burnrate can be found [16]. Results for three typical flames are shown in Fig. 3 for 50 % H_2 flames at three equivalence ratios 0.7, 1.0 and 1.5. In Fig. 3 S_n is the instantaneous flame speed dr/dt, and is normalised by S_s the flame speed at zero stretch rate ($\alpha = 0$) and α is the stretch rate which for spherically expanding flames can be shown to be [16]

$$\alpha = \frac{2}{r}\frac{dr}{dt} \qquad (4)$$

Both the experimental data and the corresponding linear least square fits are shown. The fits are used to obtain S_s and the Markstein length, L_b which is the gradient and is an indication of the influence of changes in α on the burnrate,

$$S_s - S_n = L_b\alpha . \qquad (5)$$

The laminar burning velocity, u_l is found using the flowing expression

$$u_l = S_s\frac{\rho_b}{\rho_u} \qquad (6)$$

where ρ_b and ρ_u and the burned and unburned gas densities. The flames plotted in Fig. 3 responded differently to decreasing stretch rate, the fuel lean flame slowed as it grew out from the spark whereas the flame speed of stoichiometric flame altered little. The flame speed of fuel rich flame increased dramatically and its acceleration also changed as it grew, similar behaviour has been observed in other stretch rate sensitive flames [14]. For

11

the rich equivalence ratio the assumed linear relationship between flame speed and changes in the stretch rate, from Eq. 5, is not good, but to date no better expression exists, as the changes in flame speed at $\phi = 1.5$ might be due to spark effects [15]. From these results it can be seen that the Markstein numbers given here are at best an indication of the behaviour of flame speed with stretch rate and their absolute values should be treated with circumspect.

3. Results and Discussion

At large radii the schlieren image generated a sharp outside edge to the flames that could be relatively easily detected, as shown in Figs. 1 and 2. In the early stages of flame growth and at higher u' the edge could be diffuse in appearance. In such cases it is thought that high local stretch rate resulted in a thickened reaction zone; reducing the schlieren signal, which was proportional to the local temperature gradient. At high u', portions of the flame apparently disappeared (quenched), although they could then reappear at a later time.

Previous measurements in this vessel have shown that the turbulent burning velocity of the flame continuously increased with time (and radius) throughout the measurement period [9]. This was associated with turbulent flame development. A flame can only be wrinkled by those turbulent eddies smaller than itself, with those eddies much larger than the flame bodily convecting it. On average, the proportion of turbulent eddies wrinkling the flame can be determined from the power spectral density of the turbulence field [6]. As flames grow, they are wrinkled by an increasing proportion of the turbulence spectrum and hence the "effective" u' (u'_k) increases. The relatively large integral length scale of the vessel, compared with the dimension (≈ 140 mm on average) available for monitoring turbulent flames through the windows, resulted in increasingly large eddies wrinkling the flames throughout their observed growth period.

In order to compare data from different turbulent expanding flames, u_{tr} has previously been found at a reference point where flames attain a mean radius of 30 mm [9, 10], i.e. 1.5 times the integral length scale. Choice of a smaller reference radius might result in flames still significantly influenced by the spark and subject to a small proportion of the turbulent velocity field. At high u', flames were sometimes convected away from the spark plug, thus only relatively modest flame radii could be measured before part of the kernel perimeter ceased to be visible with the result that only a limited number of measurements were obtained at high fan speeds. Selection of a mean flame radius of 30 mm was considered a reasonable compromise between these two experimental factors.

Shown in Fig. 4 are turbulent burning velocities of stoichiometric flames at a diameter of 60 mm plotted against u'. Only two of the fuels tested, CH_4 and 50% H_2, are shown for clarity. The 50 % H_2 flames propagated faster than the CH_4 flames, as expected, since the former contains faster burning hydrogen. For both fuels u_{tr} increased with increasing u' initially, but at high u' increasing turbulence did not necessarily result in a commensurate increase in burning velocity; with the consequent "bend over" in the curve fits given in the figure [6]. In the case of CH_4, no increase in u_{tr} occurred for $u' > 8$ m s^{-1}, whilst the u_{tr} for 50% H_2 continued to increase above $u' = 8$ m s^{-1}, but at a reduced rate.

There was considerable shot-to-shot variation in the measurements. This is the result of the random nature of turbulence. At ignition and as each flame grew it would have encountered turbulent eddies of varying size at different times and positions; this being particularly the case as it has already been noted that these flames were still "developing" and hence experienced only part of the total spectrum of turbulent scales at any given time. As a result, each flame was convected, and its local burn rate modified by local changes in strain rate differently, in each shot. Theoretically, when a flame becomes sufficiently large it can experience all eddies of all sizes and the burn rate will achieve a characteristic fully developed value [6]. At the reference radius employed in the present study, the flames would only have encountered a portion of the available

turbulent spectrum and so the shot-to-shot scatter observed was implicit in the measurements.

The effect of increasing the hydrogen concentration in the mixture at each u' tested is shown in Fig. 5 for $\phi = 1$. At all values of u' the burning velocity increased with hydrogen content. With the addition of 10 and 20% H_2 the rises were modest and within the shot-to-shot scatter due to the turbulence-flame interaction. By 50% H_2 significant increases in u_{tr} were observed. This was particularly evident at $u' = 8$ m s^{-1} where turbulence effects might be expected to dominate over chemical (fuel) effects.

The influence of equivalence ratio at $u' = 2$ and 6 m s^{-1} is shown in Figs.6 and 7. The symbols represent average values of the 5 or 10 shots performed at each condition (presented in this way for clarity). The average standard deviation in the results (from shot-to-shot variation) is shown by the error bars, which apply over the whole range of ϕ. The curves shown are second-order least squares fits to all measured u_{tr} data for a particular fuel. For methane, 10% H_2 and 20% H_2 the influence of hydrogen addition proved small at $u' = 2$ m s^{-1}. The burning velocity for all three fuels peaked at equivalence ratios slightly lean of stoichiometric. The lean ignition limit was also extended from 0.6 to 0.5 for 20% H_2, although there was no extension of the rich limit. The values of u_{tr} for 50% H_2 mixtures were higher than those for the three other fuels for all values of equivalence ratio, and the peak burning velocity moved slightly fuel-rich of $\phi = 1$. At $u' = 6$ m s^{-1}, shown in Fig. 7, the differences between the various fuels were more apparent. Again, methane and 10% H_2 had similar burning velocities, but the 20% H_2 was clearly faster at fuel-lean ϕ, with peak u_{tr} occurring at about $\phi = 0.8$. The 50% H_2 case again yielded faster burning at all ϕ values. The peak burning velocities occurred slightly lean of $\phi = 1$ in all cases.

Corresponding experimentally determined laminar burning velocities for all the fuels tested are shown in Fig. 8. The addition of hydrogen generally increased u_l. Pure methane flames could not be ignited beyond $\phi = 1.2$, however, the ignition limit was extended to $\phi = 1.4$ with the addition of only 10% H_2, and to $\phi = 1.6$ for 50 % H_2. The

14

addition of hydrogen did not have such a dramatic effect on the lean ignition limit; although the limit decreased from $\phi = 0.6$ to $\phi = 0.5$ in moving from pure methane to 10% H_2, it did not change further as more hydrogen was added. There was a noticeable shift in the peak burning velocity to richer ϕ with increasing hydrogen content. However, with 50% H_2 addition the peak (at about $\phi = 1.15$) still occurred significantly leaner than that for pure hydrogen (which occurs around $\phi = 1.8$ [17, 18]). It was not possible to directly compare the values of u_l derived here with those of other workers due to the higher initial temperature used in this study. Previous workers, e.g. [19], have shown reasonable agreement between their results and one-dimensional kinetic models, so shown in Fig. 9 are comparisons between measured values of u_l and those derived using Chemkin [20] computed burning velocities based on the GRI Mech 3.0 [21] and Konnov [22] mechanisms for pure methane and 50 % H_2. Burning velocities determined using the GRI Mech 3.0 proved consistently higher than those of Konnov. This is likely to reflect the experimental data used to 'calibrate' the mechanism, as the former used data primarily from counterflow burners. This experimental configuration tends to give consistently higher u_l's than those obtained using spherically expanding flames. The Konnov mechanism, compiled slightly later (when more experimentally determined laminar burning velocities were available) yielded slightly lower values of u_l. The experimental results sit between the two, except at the extremes in ϕ. For lean mixtures the Konnov mechanism matches the experiments closely. At rich ϕ the measured burning velocities are slightly larger than the computed values. This is thought to be due to the difficulty in differentiating between changes in strain and curvature effects at small radii at stretch sensitive conditions. The agreement between the experiments and the Konnov mechanism can be seen to be very close for 50 % H_2.

In addition to the laminar burning velocity, flame stretch/species diffusion effects have been recognised as having a strong influence in premixed turbulent flames [23]. These have often been characterised using a Lewis number, *Le*. The main advantage of *Le* is its simplicity as it is defined (at its most basic level) as the ratio of the species to thermal diffusion, with the species diffusion term being the diffusion of the deficient reactant in to nitrogen. However, the advantage of its simplicity is also its greatest

problem. There is a discontinuity at $\phi = 1$ where the deficient reactant changes from the fuel to oxygen, and there are difficulties in its definition when dealing with multi-component fuels. Although a combined hydrogen/methane Lewis number has been calculated Jackson *et al.* [24] it has not been widely adopted, principally because such global Lewis numbers neglect the diffusion of radicals through the flame (e.g. H, OH and O) which are important in initiating combustion by chain branching reactions [25].

The influence of changes in the stretch rate can also be expressed as a Markstein number which can be measured in counterflow or spherically expanding flames [16]. The value of the Markstein number has been shown to depend very strongly on its definition and measurement. In common with the burning velocity, it varies if measured with reference to the consumption of unburned or burned gas [26]. In addition, it has been shown that the effects of flame curvature and the rate of strain in the unburned mixture should be treated separately [14]. Combining these concepts leads to two equations involving four Markstein lengths that are required to characterize the effect of changes of stretch rate on the laminar burning rate:

$$u_l - u_{nr} = L_{cr}\alpha_c + L_{sr}\alpha_s \tag{7}$$

$$u_l - u_n = L_c\alpha_c + L_s\alpha_s \tag{8}$$

Here, u_{nr} is the burning velocity defined using the rate of production of burned gases, and u_n is defined using the rate of consumption of unburned mixture, and these quantities are different as a result of the finite flame thickness. Due to the different definitions of the burning velocity the values of the various Markstein lengths can be very different in magnitude and sign. As a result, it is at present difficult to compare values from different measurement techniques. In spherically expanding flames the magnitude of the rate of change of aerodynamic strain has been found to be significantly larger (typically 5 times) than that due to curvature, and aerodynamic strain is also thought to dominate in a turbulent flame [5]. Therefore the Markstein number (Ma_{sr}) which quantifies the influence of changes in the aerodynamic strain rate on the burning velocity, defined based on the production of burned gas, is used here as an indicator of the likely effect of

16

changes in the stretch rate that would be encountered in a turbulent flow [5]. This definition also complements the definition of turbulent burning velocity employed. It should be noted that to date there is not an accepted definition of Markstein number, Ma, for use in premixed turbulent modelling, other definitions of Ma may be quantitatively different but the trends with equivalence ratio and fuel type will be similar. Experimentally determined Markstein numbers (Ma_{sr}) plotted against ϕ are shown in Fig. 10. When measuring the Markstein number it was assumed that the influence of stretch changed the burn rate linearly, and over the range of stretch rates (flame radii) for which measurements were performed there were no other influences on the burn rate [14]. In order to meet these requirements the influence of stretch was determined over relatively large flame radii (typically 15-55 mm) to avoid spark and flame thickness effects. Even so, unaccountable oscillations and changes in flame speed have often been noted in spherically expanding flames [5, 14]. Problems with the determination of Markstein numbers became particularly severe for $\phi > 1.1$ where flame curvature (flame thickness) may also be significant [14]. As a result the uncertainty in measurements of Ma_{sr} can be large and dependent on the equivalence ratio. For these fuels, at $\phi = 0.7$ and 1.0 the estimated uncertainty was ± 0.5, however at $\phi = 1.3$ the uncertainty increased to ± 4.5. Despite this, from Fig. 10, it can be seen that for all the fuels Ma_{sr} increased with equivalence ratio. At each value of ϕ, methane had the highest Ma_{sr}, with a progressive decrease as hydrogen was added to the fuel.

In Fig. 11 values of u_{tr} are shown normalised by the corresponding value of u_l for increasing hydrogen concentration at $\phi = 1$. The best fit straight lines are effectively horizontal for all fuels; as a result, it may be concluded that for $\phi = 1$ (at any particular u') the increase in u_{tr} appears to be primarily a result of the increase in the laminar burning velocity due to hydrogen addition. To examine the influence of equivalence ratio, u_{tr}/u_l is plotted for both $u' = 2$ and 6 m s^{-1} in Fig. 12. The data for both u' have similar trends, constant u_{tr}/u_l for fuel-rich ϕ, with u_{tr}/u_l increasing as the mixtures became more fuel-lean. No differences could be distinguished between the four fuels. Similar fits have been given previously for a number of mixtures at 0.5 MPa [9,10] where it was concluded that the variation of u_{tr}/u_l with ϕ was related to that of the Markstein number.

In experiments on light hydrocarbon-air mixtures (e.g. methane) Ma_{sr} increased as the mixture moved from fuel-lean to rich, whereas u_{tr}/u_l decreased, but for iso-octane-air mixtures Ma_{sr} decreased lean to rich, whilst u_{tr}/u_l increased. The results here at 0.1 MPa are the similar as those at 0.5 MPa for methane and methane/hydrogen mixtures [10]. It follows that differences would be expected between the fuels in this study as the 50% H_2 mixtures have consistently lower measured values of Ma_{sr} compared to the other fuels, this was not observed. This could be the due the uncertainty in the determination of the Markstein number, both in inaccuracies in its measurement and its definition (Ma_{sr} might not be fully representative). A direct numerical simulation of hydrogen addition to methane at $\phi = 0.52$ has been performed [27]. Three influences of equal significance were found to account for the increase in turbulent burning velocity with hydrogen addition: (i) increased laminar burning velocity, (ii) larger flame surface area, and (iii) turbulent stretch effects on the local flame structure. Influences (ii) and (iii) were associated with thermal diffusive effects of enhanced H_2 levels in parts of the flame convex with respect to the reactants. A number of studies have concluded that hydrogen addition not only increases the burning velocity but also reduces the sensitivity of a flame to aerodynamic stretch [23, 28, 29]. The conclusions of these authors are confirmed here.

A number of researchers, e.g. [30, 31] have attempted to correlate turbulent burning velocities with turbulence parameters, typically using an expression of the form

$$u_{tr} = Bu' K^d, \tag{9}$$

where B and d are constants. In this way experimental data can be presented in a generalised form. Despite the apparent simplicity of Eq. 9 there are a number of problems when attempting to compare data from different sources. These issues stem from the fact that both u' and u_{tr} are open to interpretation. As the flames are developing they are not subject to the entire turbulent spectrum and this should be accounted for when comparing results from different experiments. Abdel-Gayed *et al.* [6] derived a non-dimensional turbulence power spectrum density function in terms of dimensionless frequency on the basis of laser Doppler measurements of isotropic turbulence in a fan stirred bomb. They assumed that the frequency band affecting flame development

extended from the highest frequency to a threshold frequency given by the reciprocal of the time elapsed from ignition. As a result, these authors developed an expression that allows the full effects of the turbulence spectrum to be accounted for in the determination of turbulent burning velocities, thereby effectively producing steady state burning velocity values. Furthermore, it has been shown that the magnitude of u_{tr} is sensitive to its derivation, with Bradley et $al.$ [7] demonstrating a large variation in the turbulent burning velocity by varying the reference radius and its definition.

The data for the stoichiometric mixtures of the current study are shown in Fig. 13 for each fuel. Empirical expressions for the turbulent burning velocity at $\phi = 1.0$ were then found; this equivalence ratio is often used in explosion modelling as it is assumed it roughly corresponds to the maximum burning velocity mixture which poses the greatest risk. Despite some shift in the peak turbulent burning velocity, those at $\phi = 1$ are close to the maximum for the range of u' and fuels tested here. Despite some scatter, the data appear to be well represented by an expression of the form of Eq. 9; as shown by the linear (log) fits. The residuals associated with the fits are given in the figure. At low values of K, u_{tr} can be seen to increase as hydrogen is added. However, as the r.m.s. turbulent velocity and value of K increases the fits for pure methane, 10% H_2 and 20% H_2 all yield similar values of u_{tr}/u'. The 50% H_2 fuel can be seen to exhibit higher u_{tr}/u' values over the whole range of K. This is likely to be associated with the lower sensitivity to variations in stretch rate (lower Lewis/Markstein number) of 50% H_2. Linear trend lines fitted to the modified data demonstrated little difference between the pure methane, 10% H_2 and 20% H_2 mixtures, although the 50% H_2 fuel had consistently greater values of u_{tr}. The correlation derived for the first three fuels is:

$$u_{tr} \quad = \quad 0.46 u_k' K^{-0.49}, \tag{10}$$

and for the 50% H_2 mixture:

$$u_{tr} \quad = \quad 0.67 u_k' K^{-0.47}. \tag{11}$$

In developing these expressions, the Karlovitz stretch factors were determined using Eq. 1. The laminar flame thickness, δ_l, was found using v/u_l, an under-estimation of the real

laminar flame thickness, but easily calculable and a good qualitative representation. The Taylor length scale, λ, was found using

$$\frac{\lambda^2}{L} = \frac{A\nu}{u'} \qquad (12)$$

where $A \approx 15$ [32]. The effective r.m.s. turbulent velocity u'_k was found from the integrated power spectral density given in Abdel-Gayed et $al.$ [6]. The ratio u'_k/u' increased from around 0.25 at $u' = 0.5$ m s^{-1} to 0.5 for $u' = 10$ m s^{-1}, therefore, the flames were not fully developed. Equations 10 and 11 are only valid over the experimental range, $0.005 < K < 1$. At low turbulence levels the burning velocity of the flame must approach the laminar burning velocity, although this form of turbulent burning velocity correlation does not predict this.

Comparison of turbulent burning velocities established in differing experiments is non-trivial, especially if quantitative agreement is required. As already noted, there are differences in the definition of the burning velocity adopted by different workers and difficulties arise in determining the extent of flame development in any given experiment. Turbulent burning velocity datasets are usually correlated in some manner. However, the correlation expressions can take a number of different forms which are not always directly comparable. A typical example is that the Damkholer number ($Da = u_l L/u'\delta_l$) is often substituted for the Karlovitz stretch factor in Eq. 9 [33, 34]. Whilst these numbers are very similar, the differing dependence of L and λ on u' results in an expression relating K and Da that depends on the experimental parameters u' and u_l. In order to compare results of a number of studies in a consistent manner, Lipatnikov and Chomiak [35] collected and reprocessed a number of databases; presenting the data using both the Damkohler and Karlovitz numbers. Karlovitz stretch factor versus u_t/u_l plots are presented for a number of existing turbulent burning velocity datasets in [35], and these are compared with Eqs. 10 and 11 in Fig. 14. Comparison is made with:
(a) The Moscow database [36], with measurements performed in a fan stirred bomb. The line represents a reduced dataset selected by Lipatnikov and Chomiak [35], limited to moderate turbulence and Le $\approx$ 1. Here u' was used.

(b) The Leeds database [4], which consists of data obtained using numerous different measurement techniques and a wide range of conditions. The following expression has been presented as a reasonably representation of the dataset:

$$u_t \quad = \quad 0.88u'_k \left(KLe\right)^{-0.3}. \tag{13}$$

for the range $0.01 < KLe < 0.63$. The line plotted in Fig. 14 is for Le =1, with values of K found using the expressions given in [4] which differ to those derived using Eqs. 1 and 13 due to the use of a differing constant.

(c) The Kido *et al.* database [37], with measurements performed in a fan stirred bomb. Again, Lipatnikov and Chomiak [35] provided a fit for a reduced database consisting of Le $\approx$ 1 flames and using u'.

(d) The Shy *et al.* [34] data, with measurements performed in a cruciform burner, with the fit again from [35] again using u'.

The correlations from previous workers are generally grouped together, indicating broad agreement between experimental databases. The absolute values of u_t/u' will depend on the definition of u_t, and so variations in u_t/u' are to be expected. Generally the gradients of the lines are similar, typically values being of the order of $u_t \sim K^{-0.3}$, although there is one exception, with the fit through the measurements of Shy *et al.* [34] having a steeper gradient. The values of u_{tr}/u_k' in Eqs. 10 and 11 are lower than those of the other studies, and the gradients are steeper than most of those of other workers. This is likely to be associated with the definition of both u_{tr} and u_k' used herein, as the magnitude of the turbulent burning velocity is particularly sensitive to its definition. It has been shown that the value of the turbulent burning can vary by a factor of as much as 5-6 with the definition of the flame radius employed, and the nature (engulfment or mass turbulent burning) of the burning velocity assumed [7].

The greater influence of K (resulting in steeper gradients in Fig. 14), and the relatively modest values of K achieved in these measurements should be examined. To obtain high values of K it is necessary to reduce the laminar burning velocity, and this is typically achieved by experimenting with fuel-lean flames. Therefore, results at higher K

21

can be obtained by using non-stoichiometric data. However, these flames have very different thermo-diffusive properties thus lean flames with lower Markstein numbers had higher values of the ratio $u_{tr}/u_k{'}$. It was therefore not felt appropriate to correlate the dataset as a whole but for ranges of Markstein number. Shown in Fig. 15 are all the data obtained in this study, separated into the three ranges of Ma_{sr} indicated in Table 1. Ranges of Ma_{sr} were used due to the aforementioned uncertainties in its measurement. Differences in behaviour for the various Markstein number ranges and $u_{tr}/u_k{'}$ can be seen, with those flames more sensitive to stretch (high Ma_{sr}) burning slower under turbulent conditions, especially at higher values of K. Also shown in Fig. 15 is the experimentally determined point of flame quench which is also dependent on Ma_{sr} and K [38]:

$$K\left(Ma_{sr} + 4\right)^{1.8} = 34.4 \qquad (14)$$

This relationship was empirically derived in the same vessel and indicates a 20% probability of a flame kernel continuing to develop. Although unlikely, it is possible for flames to burn in the indicated quench region, and indeed (for the current study) a limited number of data points can be seen in this region. From Fig. 15, it appears the quench limit was approached for all Markstein number ranges relevant to the current data.

The usefulness of the generalised form of the data presented in Fig. 15 can be tested by checking that it can predict the earlier experimental observations. It is well established that the form of Eq. 9 predicts the turndown in u_{tr} with $u{'}$ [6]. Also, flames exhibiting higher laminar burning velocities will have lower values of K (for constant $u{'}$), hence the turbulent burning velocity will be higher. In the turbulent burning velocity versus equivalence ratio data (presented in Figs. 6 and 7), 20% H_2 was only significantly faster than methane and 10% H_2 at $u{'} = 6$ m s^{-1}. This is a consequence of the divergence of the $Ma_{sr} < 2$ and $2 < Ma_{sr} < 7$ data as K increases, shown in Fig. 15. At low values of K (low $u{'}$), there are few observable differences between CH_4, 10% H_2 and 20% H_2. Differences do, however, appear at higher $u{'}$, corresponding to where the fits diverge. In Fig. 11, the ratio u_{tr}/u_l was found to be approximately uniform for each fuel as $u{'}$ was increased at $\phi = 1$. As the concentration of hydrogen was increased, values of both Ma_{sr} and K therefore decreased. At small K, Ma_{sr} has little or no influence on u_{tr}. This may be

why no increase in u_{tr}/u_l was observed as the hydrogen content was increased. Lastly, in Fig. 12, it was shown that the ratio u_{tr}/u_l increased rapidly at fuel-lean equivalence ratios, this being where Ma_{sr} is lowest and K is highest. Therefore the influence of Ma_{sr} on K is at its highest for such equivalence ratios. No such dramatic effect was observed at fuel-rich equivalence ratios where high values of Ma_{sr} and K occur, and from Fig. 15 reduced turbulent burning velocities might be expected. However, flames quench at much lower K (there is an order of magnitude difference between the ranges $Ma_{sr} < 2$ and $Ma_{sr} > 7$), and slow burning flames may not survive to a 30 mm radius. As u_{tr}/u' decreases the dependence of u_{tr} on u' is decreasing, hence the propagation rate of $Ma_{sr} > 7$ flames will (counter intuitively) be little influenced by increasingly turbulence levels (this is point at which bend over occurs [33]) although in practice these flames were observed to be heavily impacted by the turbulence with the flames suffering from localised quenching and often convected around the vessel in their early stages. This could lead to significant problems in practical combustion devices.

The findings resulting from this work remain contradictory. The addition of hydrogen to methane results in a more reactive faster burning fuel, this has been demonstrated by a number of previous studies ([2],[3], [19]. [24] to reference a few) and is confirmed here in both laminar and turbulent conditions. However, it is not clear how significant flowfield stretch effects are on turbulent premixed flames, there is evidence here that they can be neglected but also some plots show that they may be significant. Part of the problem stems from the difficulties of defining and measuring the influence of changes in the stretch rate in laminar flames (given as a Markstein number), this data should be treated with circumspection and remains a qualitative measure. It can be said that for the mixtures used here lean flames were less sensitive to changes in the stretch rate than rich ones, and this can be demonstrated to have an influence in turbulent flames, as shown in Fig. 12. The addition of hydrogen reduced the Markstein number but this did not seem to have much influence in turbulent flames for $\phi = 1.0$ (see Fig. 11) where the increase in u_l with hydrogen appeared to be primary reason of increases in u_{tr}. Turbulent burning velocity correlations (of K vs. u_{tr}/u'_k) were used in an attempt to summarise the whole dataset and compare these measurements with those of other workers. However differences in the definitions of the turbulent burning velocity and the treatment of

turbulent flame development mean that it is difficult to draw concrete conclusions between studies. The measurements obtained here were qualitatively similar to those of other workers. For stoichiometric flames the 50 % H_2 could not be fitted with the other fuels and this is attributed to differences in the response of the flame to changes in the stretch rate. However a much more dramatic influence of Markstein number was again shown when measurements over the whole range of ϕ were included. The fuel lean flames were much less sensitive to increasing stretch rate, given by K, than the fuel rich flames, with the differences between the flames being most apparent at high values of K.

4. Conclusions

Methane and methane-hydrogen (10%, 20% and 50% hydrogen by volume) mixtures have been ignited in a fan stirred bomb in turbulence and the resultant turbulent burning velocity, u_{tr}, measured at a flame radius of 1.5 integral length scales of turbulence for a range of r.m.s. turbulent velocities. Corresponding laminar burning velocities have also been measured for the same mixtures. The main conclusions of this work are:

- The addition of 10% hydrogen did not result in a significant increase in u_{tr}. For 20% hydrogen there was a clear increase in u_{tr} for lean equivalence ratios, but not for rich. In the case of the addition of 50% hydrogen there was an increase in u_{tr} for all ϕ. Both the fuel-lean and rich ignition limits were extended with the addition of hydrogen.

- The addition of hydrogen resulted in an increase in the measured laminar burning velocity, u_l, and a decrease in the Markstein number, Ma_{sr}.

- For stoichiometric mixtures the ratio u_{tr}/u_l did not change with the addition of hydrogen for a constant u'.

- The ratio u_{tr}/u_l increased as the mixtures became leaner for constant u'. For the leanest mixtures u_{tr}/u_l could be 3-4 times that observed for the stoichiometric case. This was the result of lean flames being less sensitive to stretch rate, as exhibited in lower values of Ma_{sr}.

- Non-dimensional plots (u_{tr}/u_l against K, the Karlovitz stretch factor) showed that the addition of 50% hydrogen results in faster burning than for the other fuels for all

- The influence of flame thermo-diffusive effects on the turbulent burning velocity increased as K is increased.

- Non-dimensional correlations of turbulent burning velocity data, corrected to fully developed turbulent flow conditions, have been produced for use in mathematical models for the prediction of explosion overpressures.

25

References

1. A. Züttel, A. Borgschulte, L. Schlapbach (Eds.), Hydrogen as a Future Energy Carrier, Wiley-VCH, Weinheim. 2008.

2. Z. Huang, Y. Zhang, K. Zeng, B. Liu, Q. Wang, D. Jiang, Combust. Flame 146 (2006) 302-311.

3. V. Di Sarli, A. Di Benedetto, Int. J. Hydrogen Energy 32 (2007) 637-646.

4. D. Bradley, A.K.C. Lau, M. Lawes, Phil. Trans. R. Soc. London 338 (1992) 359-387.

5. L. Gillespie, M. Lawes, C.G.W. Sheppard, R. Woolley, Aspects of Laminar and Turbulent Burning Velocity Relevant to SI Engines, SAE Paper 010192 (2000).

6. R.G. Abdel-Gayed, D. Bradley, M. Lawes, Proc. R. Soc. Lond. A 414 (1987) 389-413.

7. D. Bradley, M.Z. Haq, R.A. Hicks, T. Kitagawa, M. Lawes, C.G.W. Sheppard, R. Woolley, Combust. Flame 133 (2003) 415-430.

8. C. Morley, GASEQ: A Chemical Equilibrium Program for Windows Program, see www.gaseq.co.uk (2001).

9. M. Lawes, M.P. Ormsby, C.G.W. Sheppard, R. Woolley, Combust. Sci. Technol. 177 (2005) 1273-1289.

10. C. Mandilas, M.P. Ormsby, C.G.W. Sheppard, R. Woolley, Proc. Combust. Inst. 31 (2007) 1443-1450.

12. D. Bradley, R.A. Hicks, Lawes, M., and Sheppard, C. G.W., Engine and Fuel Interaction In Real Engines, Final Report CEC Contract JOU-2-CT92-0162, Commission of the European Communities and Daimler-Benz AG, Brussels, 1996.

11. K. Nwagwe, H.G. Weller, G.R. Tabor, A.D. Gosman, M. Lawes, C.G.W. Sheppard, R. Woolley, Proc. Combust. Inst. 28 (2000) 59-65.

13. F. Atzler, Fundamental Studies of Aerosol Combustion, Ph.D. Thesis, University of Leeds, UK (1999).

14. D. Bradley, R.A. Hicks, M. Lawes, C.G.W. Sheppard, R. Woolley, Combust. Flame 115 (1998) 126-144.

15. A.A. Burluka, M. Fairweather, M.P. Ormsby, C.G.W. Sheppard and R. Woolley, The Laminar Burning Properties of Premixed Methane-Hydrogen Flames Determined Using a Novel Analysis Method, ECM 2007.

16. P. Clavin, Prog. Energy Combust. Sci. 11 (1985) 1-59.

17. C.K. Wu, C.K. Law, Proc Combust. Inst. 20 (1984) 1941-1949.

18. X. Qin, H. Kobayashi, T. Niioka, Exp. Therm. Fluid. Sci. 21 (2000) 58-63.

19. F. Halter, C. Chauveau, N. Djebaïli-Chaumeix, I. Gökalp, Proc. Combust. Inst. 30 (2005) 201-208.

20. R.J. Kee, J.F. Grgar, M.D. Smooke, J.A. Miller, A Fortran Program for Modeling Steady Laminar One-Dimensional Premixed Flames, Report No. SAND85-8240, Sandia National Laboratories, 1985.

21. P.G. Smith, D.M. Golden, M. Frenklach, N.W. Moriarty, M. Goldenberg, C.T. Bowman, R.K. Hanson, S. Song, W.C. Gardiner Jr., V.V. Lissianski, Z. Oin, from http://www.me.berkeley. edu /gri_mech/.

22. A. Konnov, Release 0.4, from http://homepages.vub.ac.be/~akonnov/, 1998.

23. A.N. Lipatnikov, J. Chomiak, Prog. Energy Combust. Sci. 31 (2005) 1-73.

24. G.S. Jackson, R. Sai, J.M. Plaia, C.M. Boggs, K.T. Kiger, Combust. Flame 132 (2003) 503-511.

25. J.F. Griffiths, J.A. Barnard, Flame and Combustion, 3 Ed. Blackie A & P, 1995.

26. J. H. Tien, M. Matalon, Combust. Flame 84 (1991) 238-248.

27. E. R. Hawkes , J. H. Chen, Combust. Flame 138 (2004) 242-258.

28. G. Yu, C.K. Law, C.K. Wu, Combust. Flame 63 (1986) 339-347.

29. J.-Y. Ren, W. Qin, F.N. Egolfopoulos, T.T. Tsotsis, Combust. Flame 124 (2001) 717-720.

30. K.N.C. Bray, Proc. R. Soc. Lond. A 431 (1990) 315-335.

31. O.L. Gülder, Proc Combust. Inst. 23 (1991) 743-750.

32. V. Sick, M.R. Hartman, V.S. Arpaci, R.W. Anderson, Combust. Flame 127 (2001) 2119-2123.

33. N. Peters, Turbulent Combustion, Cambridge University Press, 2000.

34. S.S. Shy, W.J. Lin, J.C. Wei, Proc. R. Soc. Lond. A 456 (2000) 1997-2019.

35. A.N. Lipatnikov, J. Chomiak, Prog. Energy Combust. Sci. 28 (2002) 1-74.

36. V.P. Karpov, E.S. Severin, Combust. Explos. Shock Waves 16 (1980) 41-46.

37. H. Kido, T. Kitagawa, K. Nakashima, K. Kato, Mem. Faculty Engng., Kyushu Univ 49 (1989) 229-247.

38. D. Bradley, M. Lawes, K. Liu, R. Woolley, Proc. Combust. Inst. 31 (2007) 1393-1400.

Fuel	$Ma_{sr} < 2$	$2 < Ma_{sr} < 7$	$Ma_{sr} > 7$
CH_4	-	$0.6 \leq \phi \leq 1.1$	$\phi \geq 1.2$
10% H_2	$\phi \leq 0.7$	$0.8 \leq \phi \leq 1.1$	$\phi \geq 1.2$
20% H_2	$\phi \leq 0.8$	$0.9 \leq \phi \leq 1.2$	$\phi \geq 1.3$
50% H_2	$\phi \leq 1.1$	$1.2 \leq \phi \leq 1.3$	$\phi \geq 1.4$

Table 1. Data contained in the Ma_{sr} ranges shown in Figure 15.
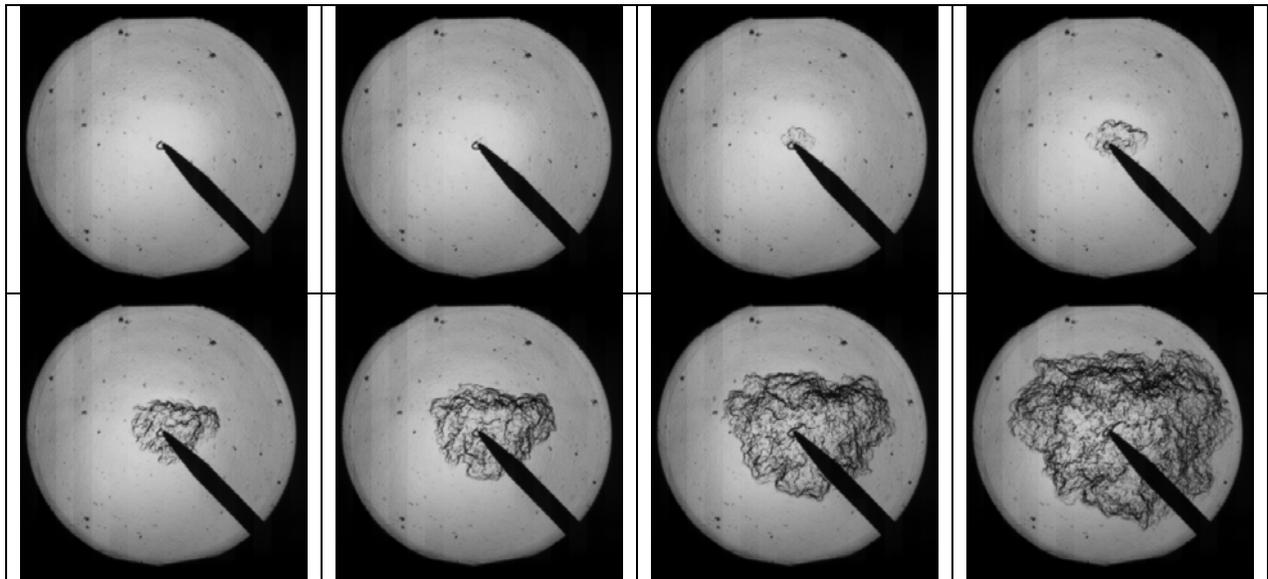
Figure 1. Turbulent flame propagation of a typical, turbulent $\phi = 1$, 50% H_2 flame at $u' = 6$ m s^{-1} (images at 2 ms intervals).
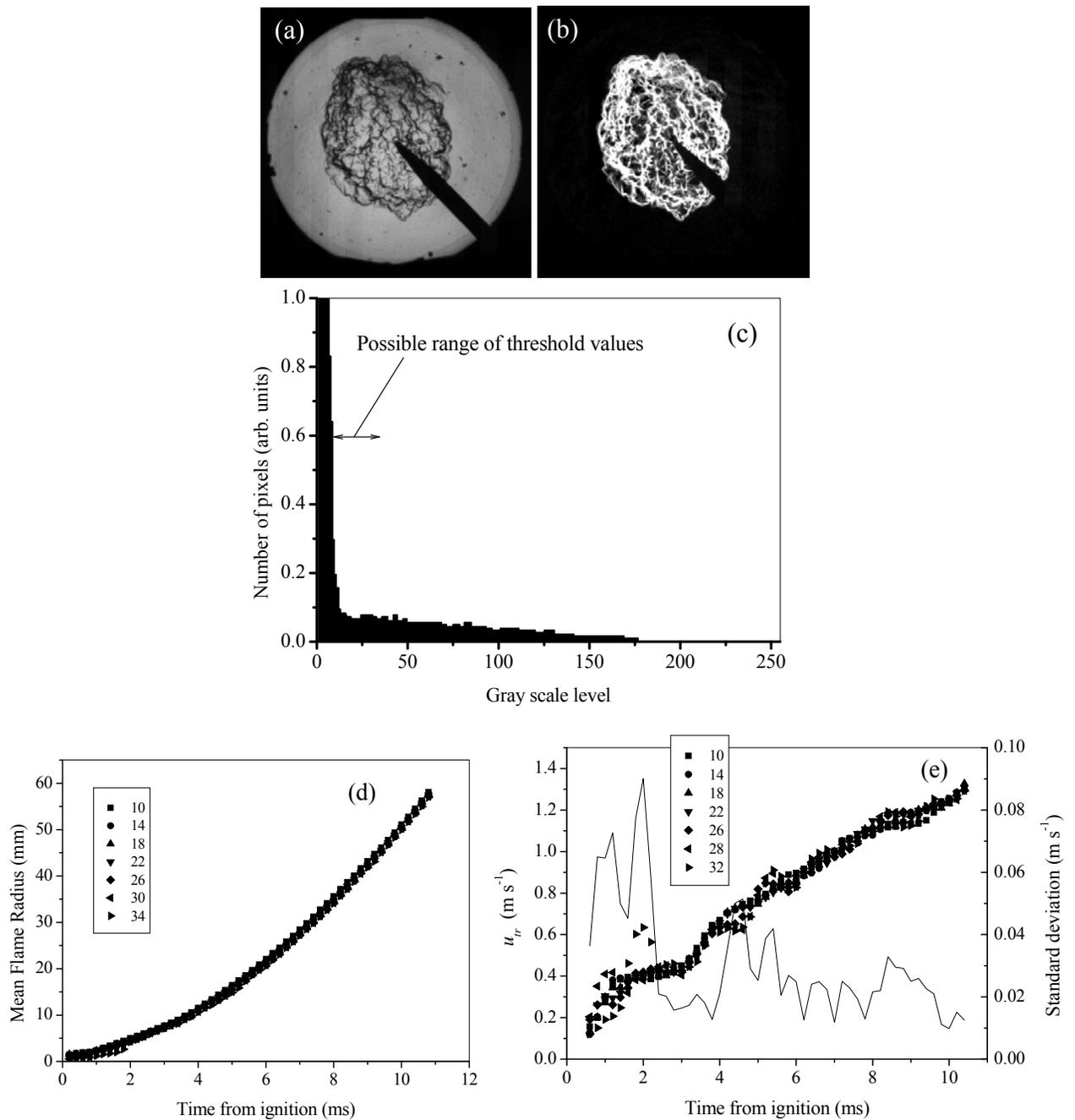
Figure 2. Flame processing procedure for a typical flame (CH$_4$/air, $\phi = 0.9$, $u' = 2$ m s^{-1}): (a) original schlieren image, (b) image after background subtraction, (c) image histogram after background subtraction, (d) flame radius against time from ignition for different grey scale threshold values, and (e) turbulent burning velocity against time from ignition, with the standard deviation in the velocities found at the various threshold values also shown.
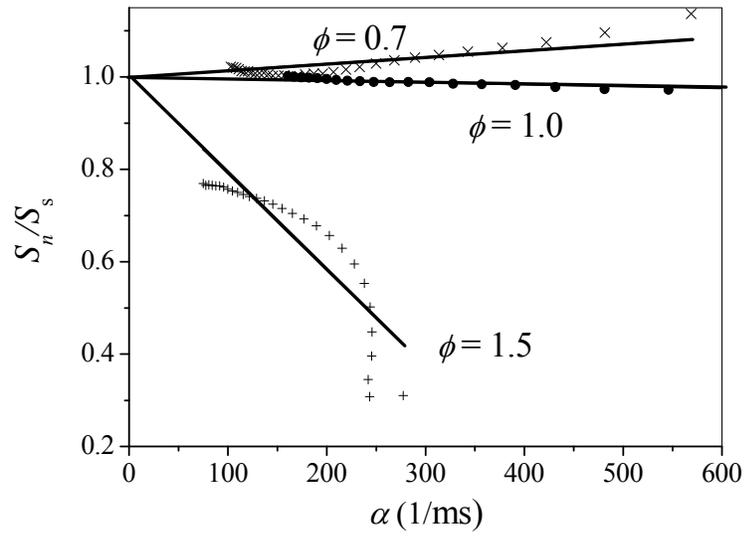
Fig. 3. Normalised laminar flame speed vs. flame stretch rate for three typical 50 % H_2 flames.
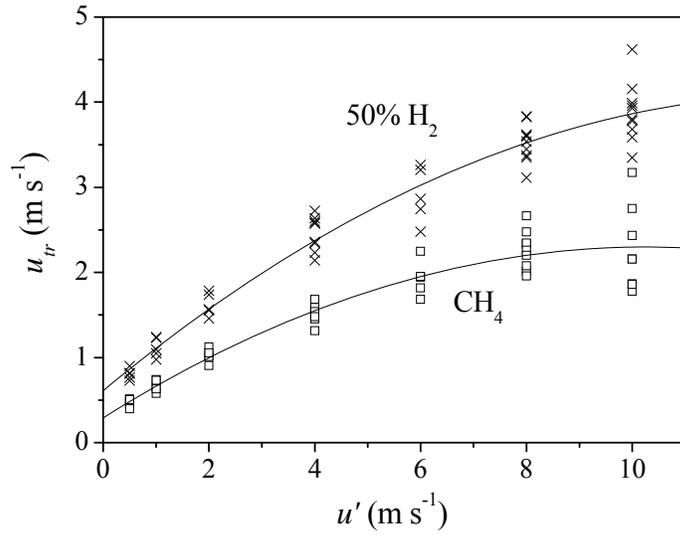
Figure 4. Turbulent burning velocities, u_{tr}, against u' for CH$_4$ and 50% H$_2$ at $\phi = 1$.
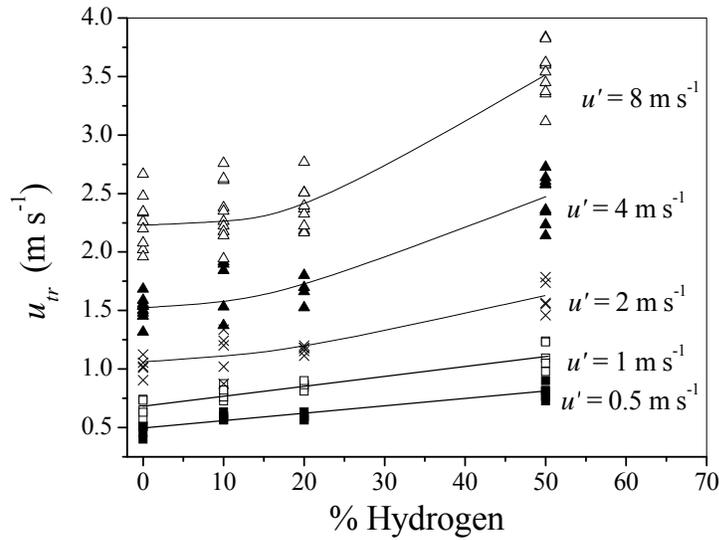
Figure 5. Turbulent burning velocity against percentage hydrogen in the fuel with u' for $\phi = 1$.
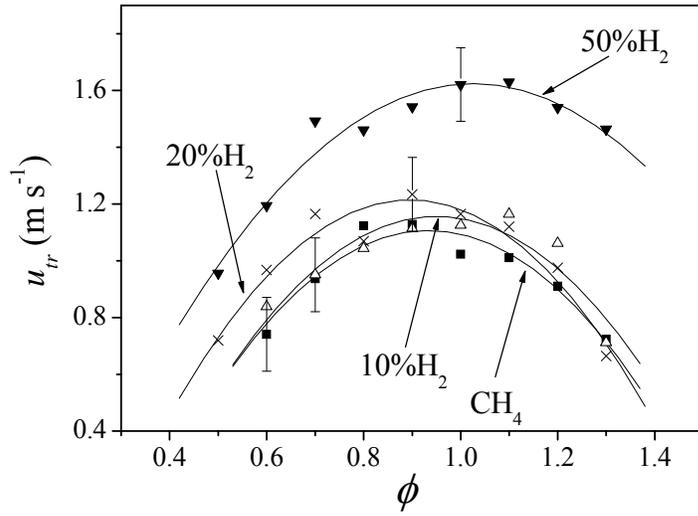
Figure 6. Average turbulent burning velocities against equivalence ratio for all fuels at $u' = 2$ m s^{-1}, including second-order least square fits to data.
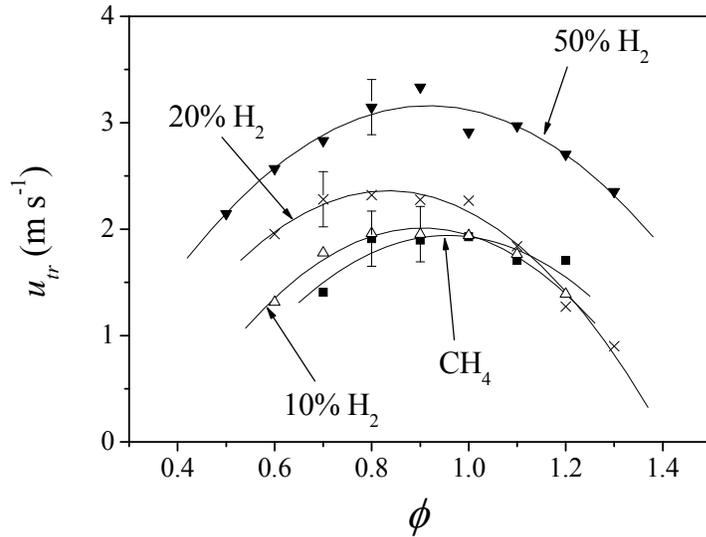
Figure 7. Average turbulent burning velocities against equivalence ratio for all fuels at u' = 6 m s^{-1}, including second-order least square fits to data.
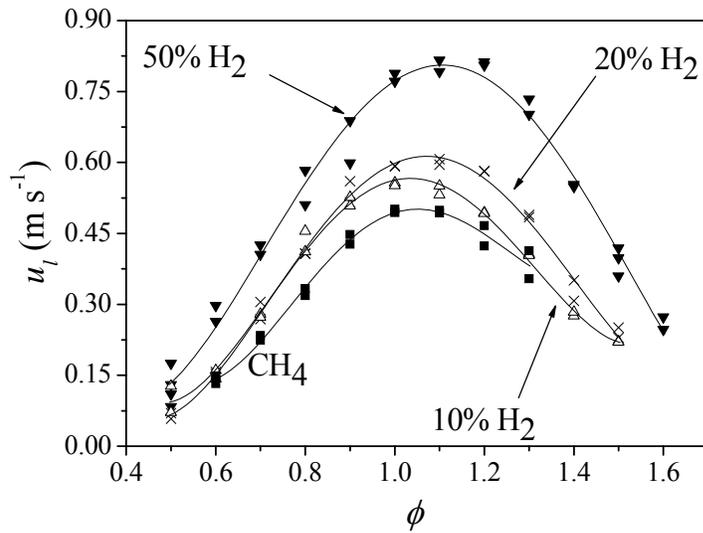
Figure 8. Measured unstretched laminar burning velocity against equivalence ratio for all fuels.
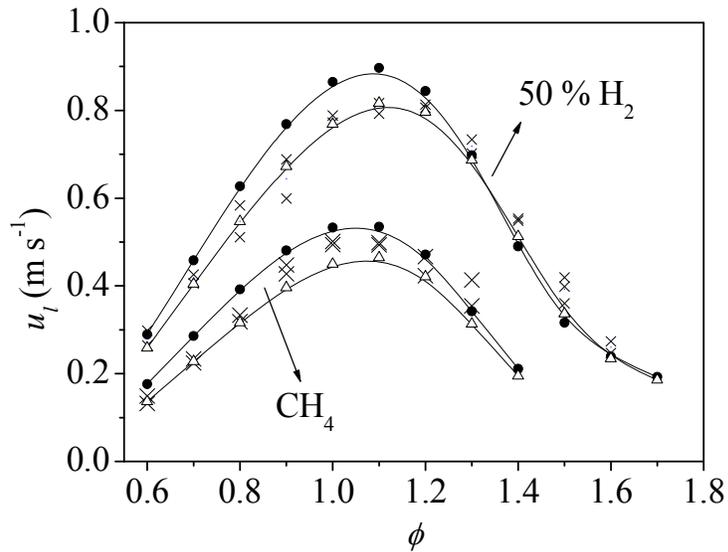
Figure 9.   Comparison of experimental and computed laminar burning velocities for methane and 50 % hydrogen addition (crosses – data, triangles – GRI Mech 3.0, filled circles – Konnov).
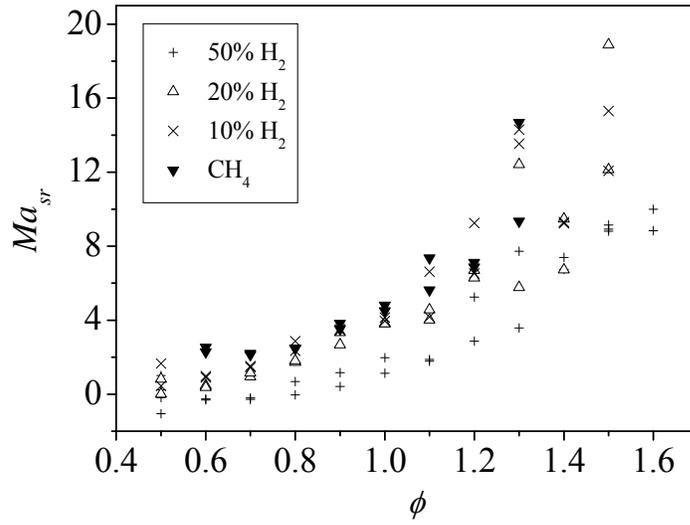
Figure 10. Markstein lengths against equivalence ratio for all fuels.
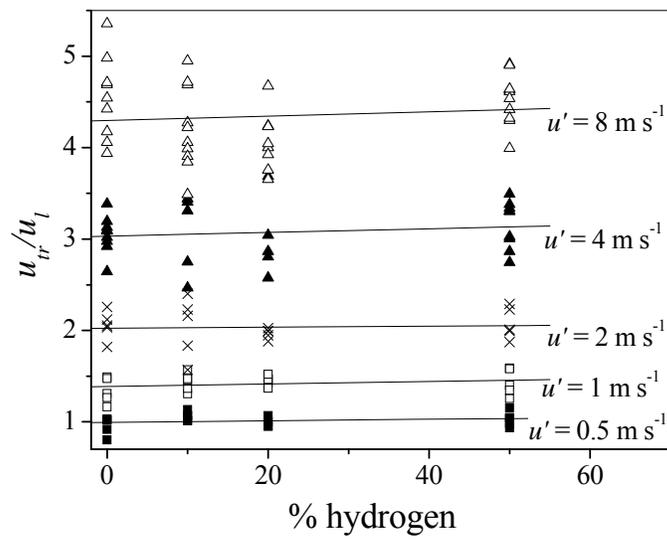
Figure 11. The ratio u_{tr}/u_l against percentage hydrogen in the fuel with u' for $\phi = 1$.
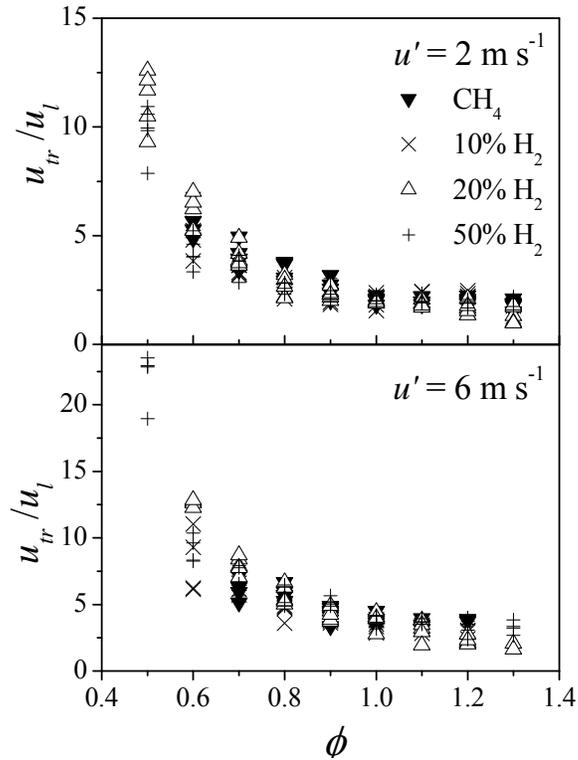
Figure 12. The ratio u_{tr}/u_l against equivalence ratio for all fuels at $u' = 2$ and 6 m s^{-1}.
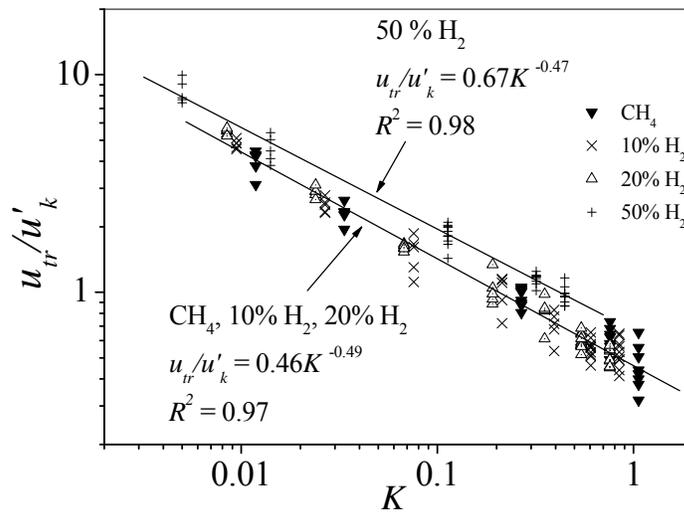

Figure 13. Values of u_{tr}/u'_k plotted against K for stoichiometric mixtures over a range of u', with data for different fuels shown.

36
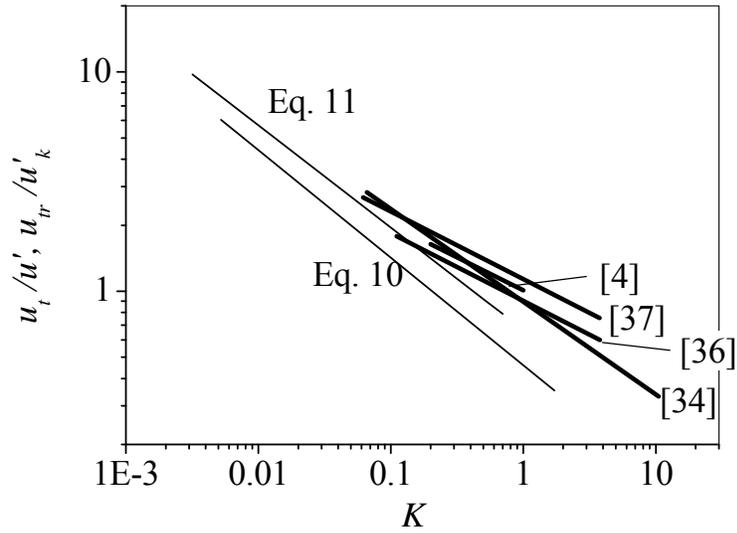
Figure 14.   Comparison between the best fits derived in this study and the turbulent burning correlations of other workers.
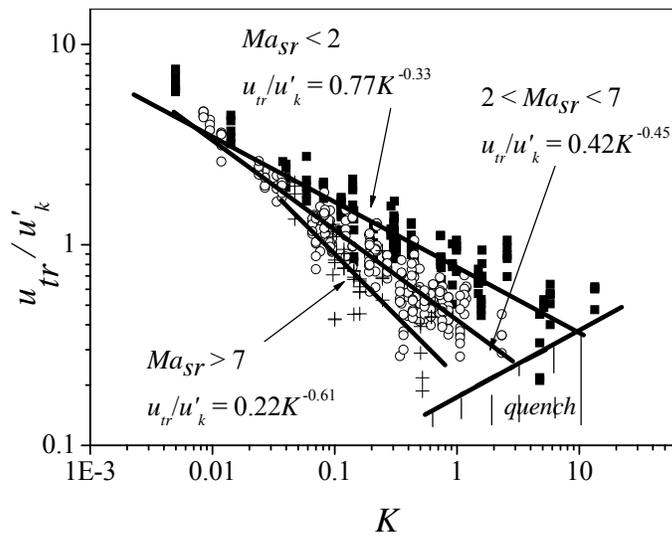
Figure 15.   Values of u_{tr}/u'_k plotted against K for all measurements, with data for different ranges of Ma_{sr} shown ($Ma_{sr} < 2$ – filled squares, $2 < Ma_{sr} < 7$ – open circles, $Ma_{sr} > 7$ crosses).